Applied Acoustics 145 (2019) 60–68

Contents lists available at ScienceDirect

Applied Acoustics

journal homepage: www.elsevier.com/locate/apacoust

# Accuracy of vibro-acoustic computations using non-equidistant frequency spacing

Matthias Klaerner [a,*], Mario Wuehrl [a], Lothar Kroll [a,b], Steffen Marburg [c]

[a] Institute of Lightweight Structures, Chemnitz University of Technology, 09107 Chemnitz, Germany
[b] Institute of Mechanics, Opole University of Technology, 45758 Opole, Poland
[c] Gerhard Zeidler Endowed Professorship for Vibroacoustics of Vehicles and Machines, Technische Universität München, 85748 Garching, Germany

ARTICLE INFO

*Article history:*
Received 21 November 2017
Received in revised form 24 August 2018
Accepted 12 September 2018
Available online 1 October 2018

*2010 MSC:*
00-01
99-00

*Keywords:*
Sound radiation
Structure borne sound
Approximation methods
Finite Element Analysis
Equivalent radiated sound power
Lumped parameter model

ABSTRACT

Within the vibro-acoustic optimisation of complex components under dynamic loading the radiated sound power is commonly used as an objective. For this purpose, the frequency-dependent sound power has to be quantified by a single scalar objective. For the required steady state simulations the mode-based frequency spacing can include non-equidistant step sizes as well as can change due to structural or material modifications. Thus, the total number of frequency steps is depending on the number of contributing modes that can be changed during optimisation processes with structural or material modifications. Furthermore, the accuracy of the objective has to be assured by choosing the required number of frequency steps and avoiding either under-resolved peaks or too many frequency steps.

In this study, we present an approach for the determination of the averaged sound power within the covered frequency range with non-equidistant spacing based on the power spectral density. These scalar quantities are robust to any model changes. Thereafter, the mean power is used as a convergence criterion to determine the number of required frequency steps for a single mode and thus to reduce the computational efforts to a minimum.

Further, a recommendation for a common rule for the spacing of single mode is given. This results in the frequency spacing estimation depending on the distance of neighbouring modes as well as the damping and biasing. Moreover, the combination of robust scalar objectives and efficient frequency spacing opens the prospects of accessing sound power objectives for complex optimisation problems.


## 1. Introduction

Lightweight components are typically thin-walled and stiff and thus tend to be sensitive for significant sound radiation. In addition, fibre-reinforced plastics (frp) with a wide range of adjustable material properties such as stiffness and even damping induced by manipulating layup, fibre/matrix material or fibre volume content are used.

Due to the acoustic sensitivity of stiff and thin-walled structures the sound radiation behaviour is a common optimisation objective within lightweight design [1–3]. Furthermore, the design of quiet structures implies a large potential of structural-acoustic optimisation. Fast frequency response analysis as well as its numerous repetitions with different parameter sets are a key issue in efficient optimisation processes [4,5].

Within these optimisation processes, the radiated sound power is used to express the radiation of components and machines and is formulated as the integral of the intensity over the radiating surface. Analytical solutions of sound power are limited to a few cases with regular geometries [6–8]. In addition, precise numerical approximation methods solving fluid–structure-interaction in one or both directions are used but are computationally expensive. Furthermore, the boundary element method (BEM) including fast-multipole techniques is a very popular approach for large-scale problems but is limited in applications with a large frequency range or modified structures within optimisation loops, e. g. [9].

In between fast analytical solutions of simple structures and computationally expensive BEM models are different approaches based on structural dynamic finite element analysis (FEA) using the surface velocity of the component. Particularly, there is the equivalent radiated power (ERP) as well as the more precise lumped parameter model (LPM) [10].

* Corresponding author.
*E-mail address:* matthias.klaerner@mb.tu-chemnitz.de (M. Klaerner).

https://doi.org/10.1016/j.apacoust.2018.09.008
0003-682X/

These simplification methods are based on some of the following general assumptions. Stiff thin-walled structures with hard reflecting surfaces show identical particle velocity and normal structure velocity. Here, the sound pressure is evaluated on the structure's surface [10,11]. Last, the kinetic energy is implicitly given in steady state FEA solutions and thus provides information about the dynamic behaviour without any additional efforts. Possibilities and limits of estimating the radiated sound power by these methods have been shown by numerical studies on a composite component [12]. Moreover, the total power as an integral over frequency is used to demonstrate the feasibility and accuracy of such optimisation objectives.

As stiffness and damping are contradictorily influenced by fibre volume content, fibre orientation as well as stacking sequence optimising the material properties of frp results in non-linear dependencies [13,14]. In addition, composites show significant uncertainties in fibre orientation [15]. Thus, numerous finite-element simulations may be required either for genetic or gradient based optimisations. In summary, there is a need for efficient numerical quantities of structure-borne sound radiation of such processes [16].

Additionally, frequency domain structural dynamic FEA with modal superposition can be used to integrate anisotropic damping of composites by using an energy related approach [17–20] and is thus suitable for acoustic laminate optimisations. Moreover, the previous modal analysis can be used for a mode-based frequency spacing. This assures an accurate representation of the resonances but leads to non-equidistant frequency steps. The total number of frequency steps depends on the number of modes within the treated frequency range. Changing geometry or material parameters within optimisation procedures may result a varying number of contributing modes and thus different frequency stepping.

Reducing the radiated sound power by numerical optimisation methods requires a robust objective [4,21], typically as a scalar value. This reduction of information is in contrast to the strong dependency of the radiated sound power on the frequency wherein resonances contribute the most. Thus, a frequency-dependent assessment of the final design in relation to the excitation spectra is required.

Within this study, an approach to determine the average power in the given frequency range based on the power spectral density is presented. It is based on a subdivision of the sound intensity within the total bandwidth into small frequency intervals wherein only small changes of intensity appear [22]. The determination is independent of the number of modes and frequency steps and valid for varying frequency step sizes. This enables the comparison of different components, materials or geometries as well as the implementation as an optimisation objective.

Thereafter, the mean power is used as a convergence criterion to determine the number of required frequency steps for a single mode and thus to reduce the computational efforts to a minimum. As a result, the frequency spacing can be estimated depending on the distance of neighbouring modes as well as the damping and biasing.

## 2. Theoretical background of FEA-based sound power quantification

### 2.1. Structural FEA-based sound power approaches

The radiated sound power $P$ is commonly used to quantify the structure-borne sound of vibrating parts. It is an integral of sound intensity $I$ in normal direction over a closed surface $\Gamma$ circumscribing the radiating object [10]

$$P = \int \vec{I} \cdot \vec{n} \, \mathrm{d}\Gamma \quad \text{with} \quad \vec{I} = \frac{1}{2}\Re(p\vec{v}^*) \tag{1}$$

wherein $*$ denotes a conjugate complex value as well as $\Re$ the real part of a complex state variable. The velocity normal to the surface $v_n = \vec{v} \cdot \vec{n}$ is determined by steady state structural dynamic FE-analysis. Hence, a simple, popular and efficient approach for the sound pressure in local relation is

$$\boldsymbol{p} \approx \rho_f \, c_f \boldsymbol{v}_n \tag{2}$$

with the fluid's density $\rho_f$ as well as its speed of sound $c_f$. The relation between particle velocity and sound pressure is reduced to the fluid's characteristic impedance

$$Z_0 = \rho_f \, c_f. \tag{3}$$

The approximation by the equivalent radiated sound power (ERP) is typical in far fields and high frequencies and results in the sound power as a surface integral

$$P_{ERP} = \frac{1}{2}\rho_f \, c_f \int_\Gamma |\boldsymbol{v}_n|^2 \mathrm{d}\Gamma \tag{4}$$

which is eqivalent to a radiation efficiency of $\sigma = 1$ or a discretised formulation for $N_e$ constant elements with an area $S_\mu$

$$P_{ERP} = \frac{1}{2}\rho_f \, c_f \sum_{\mu=1}^{N_e} S_\mu v_{n_\mu} v_{n_\mu}^*. \tag{5}$$

This simple formulation is based on the assumption of the same radiation efficiency $\sigma = 1$ for all elemental sources. It neglects effects such as interaction between local sources. Generally overestimating the radiation, it gives a good impression of an upper bound for convex rigid bodies and high frequencies.

The most accurate approximation is the lumped parameter model (LPM) by KOOPMANN and FAHNLINE [23–25]. It is a simplification of the RAYLEIGH-integral including a TAYLOR series for the GREEN's function as a multi-pole expansion. This yields to a formulation for a source at $x_\mu$ and a receiver at $y_v$

$$P_{LPM} = \frac{1}{2}k \, \rho_f \, c_f \sum_{\mu=1}^{N_e}\sum_{v=1}^{N_e} S_\mu S_v \frac{\sin(k|x_\mu - y_v|)}{2\pi|x_\mu - y_v|} \Re\{v_\mu v_v^*\} \tag{6}$$

also considering the interactions of the elemental sources. With the wave number $k$ it includes a frequency-dependent radiation efficiency. The LPM predictions are exact for dipole modes. Besides, it already provides appropriate results in the low and mid frequency range.

In summary, the FEA-implementation of the sound power approximations is based on piecewise constant elements.

$$P = \sum_{\mu=1}^{N_e}\sum_{v=1}^{N_e} P_{\mu v} = \sum_{\mu=1}^{N_e} P_{\mu\mu} + 2\sum_{\mu=1}^{N_e-1}\sum_{v=\mu+1}^{N_e} P_{\mu v} \tag{7}$$

The sound power portions $P_{\mu v}$ are understood as a partial sound power of all $N_e$ constant elements acting as a monopole source. In detail, $P_{\mu\mu}$ considers the independent source distributions whereas $P_{\mu v}(\mu \neq v)$ represents the interaction between these sources.

The matrix is symmetric and its elements can be determined by

$$P_{\mu v} = P_{v\mu} = \frac{1}{2}\rho_f \, c_f \, S_\mu \, \sigma_{\mu v} \, \Re\{v_\mu v_v^*\} \tag{8}$$

with the dimensionless radiation efficiency $\sigma_{\mu v}$. It gives a good impression of the different considerations of local effects and frequency-dependency. For the different sound power models $\sigma_{\mu v}$ acts as

$$\sigma_{\mu v} = \delta_{\mu v} \qquad \text{for ERP}, \tag{9}$$

$$\sigma_{\mu\nu}(f) = \frac{k^2\ S_v}{2\ \pi} \frac{\sin(k\ |x_\mu - y_v|)}{k\ |x_\mu - y_v|} \qquad \text{for LPM.} \tag{10}$$

Concerning accuracy and efforts, there are more FEA-based approaches between ERP and LPM, which are not explained in detail here. Weighting functions for the ERP are used to reduce low frequency deviations [12,26]. In addition, the volume velocity is a simplification of the LPM and appropriate for low and mid frequencies only [10,12].

In acoustics, the power levels are related to a reference of $P_0 = 10^{-12} W$

$$L_W = 10\ \lg\left(\frac{P}{P_0}\right)\ dB. \tag{11}$$

### 2.2. Energetic quantities in steady state FEA

The energy balance is estimated inherently within steady state finite element simulations and consists of different elastic and dissipating components. By solving the energy balance, the kinetic energy is directly accessible without any additional post-processing efforts. Thus, the kinetic energy of the whole system or several components is given by the integral over the volume $V$

$$E_{kin} = \int_V \frac{1}{2}\rho_s\ \boldsymbol{v}^H \boldsymbol{v} \mathrm{d}V \tag{12}$$

with the density of the solid surface $\rho_s$ and the arbitrarily oriented velocity $\boldsymbol{v}$ [27].

For thin-walled components the sound radiation is dominated by out-of-plane waves. Thus, the displacement characteristics are reasonably assumed to be basically in surface normal direction. As kinetic energy and all previous sound power estimates depend on the second order of the velocity, these global quantities are suitable to determine the acoustic radiation behaviour [12,23].

Steady state FEA assures pure harmonic vibrations in every single frequency step. The provided solutions are thus point-wise exact. The kinetic energy can further be rated as the mechanical (input) power of the whole vibrating system [12].

$$P_{kin}(f) = 2\pi \cdot \mathrm{f} \cdot E_{kin}(f) \tag{13}$$

### 2.3. Scalar sound quantification standards

Sound radiation is strongly depending on frequency with most relevant contributions at the resonances. Changing material or geometry in optimisation processes may result in a different number of modes contributing within the considered frequency range $(f_u - f_l)$.

In contrast to the given complex frequency-dependent quantities, scalar values are more likely to be implemented as an objective within numerical optimisations [16,28]. Therefore, the mean power within the treated frequency range is determined by

$$\overline{P} = \frac{1}{(f_u - f_l)} \int_{f_l}^{f_u} P(f) df = \frac{1}{(f_u - f_l)} \sum_{n=1}^{N_f} (\mathrm{d}f_n P_n) \tag{14}$$

and is estimated by a frequency integral over all $N_f$ frequency steps with

$$\mathrm{d}f_n = \frac{f_{n+1} - f_{n-1}}{2} \qquad \text{for} \qquad 2 \leqslant n \leqslant N_f - 1 \tag{15}$$

$$\mathrm{d}f_1 = \frac{f_2 - f_1}{2} \tag{16}$$

$$\mathrm{d}f_{N_f} = \frac{f_{N_f} - f_{N_f - 1}}{2} \tag{17}$$

referring to Fig. 1. It represents the same area under the curve within $(f_u - f_l)$ as the frequency-dependent approaches. The mean sound power level $L_{\overline{W}}$ is defined by (11).

This mean power determination with non-equidistant frequency steps is required to develop guidelines for an appropriate and efficient frequency spacing in the following sections.

It should be mentioned, that this idea similar to adaptive integration [29] and can be further extended using Gauss-Legendre-quadrature or the adaptive Simpson quadrature routine [30,31].

## 3. Example of problem: sound radiation of a rectangular plate

### 3.1. Model description

For an FEA parameter study, a model of a free-free rectangular plate of $278 \times 234 \times 2\ \mathrm{mm}^3$ with 1600 quadratic shell elements (4961 nodes) has been used [32]. Linear isotropic material behaviour has been considered ($E = 200\ \mathrm{GPa}, \nu = 0.3, \rho = 7.89\ \mathrm{g/cm}^3$) and a viscous damping ($D = 0.0001$) implied. The plate is excited in normal direction with 1 N at an arbitrary point apart from diagonals or symmetry axes.

With an aspect ratio of 1:1.188 and the given dimensions the plate is tuned to have its first (torsion) mode at 100 Hz as well as a maximum frequency difference of the first five modes (Fig. 2) within the range up to 300 Hz. Higher in frequency, the modal density typically is increasing, which is illustrated by the increasing number of modes per third octave band (blue) as well as the modal frequencies appearing more closely (red).

### 3.2. Frequency spacing control in steady state simulations

The number and distribution of the frequency steps can be controlled by different parameters within steady state FEA. Using ABAQUS v. 6.14 during this study, its given frequency spacing options

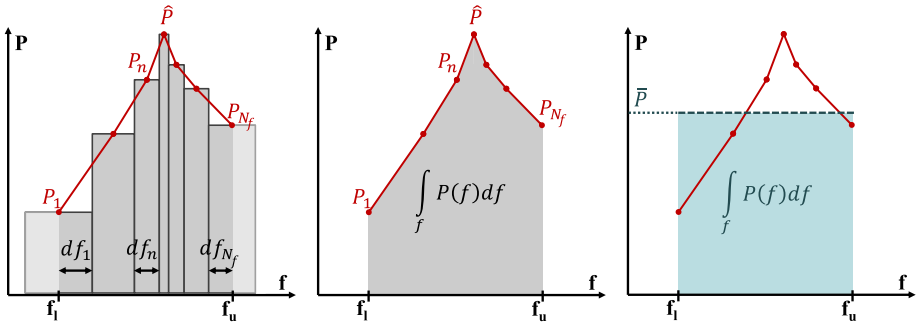


**Fig. 1.** Frequency integral approach (left): determination of the surface integral (centre) and mean power (right).

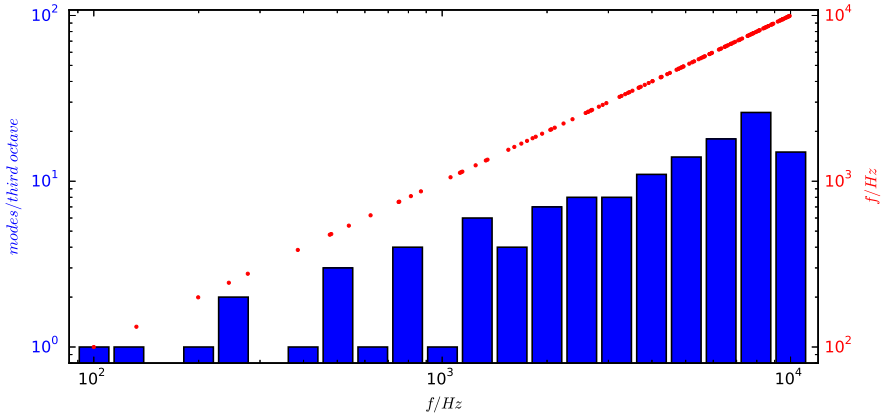


**Fig. 2.** Modal analysis of a rectangular plate: eigenfrequencies (red) and number of modes per third octave band (blue). (For interpretation of the references to colour in this figure legend, the reader is referred to the web version of this article.)

are state of the art and further compared to show their restrictions considering accuracy and numerical efforts.

For illustration of the different frequency step options FEA models with 55 frequency steps in a range from 10 Hz to 350 Hz have been used covering the first five modes of the plate (noted with vertical lines). Fig. 3 (top) shows the sound power results with a shift of 50 dB between the curves due to readability. Each curve is overlaying an accurate solution with a very high frequency resolution of 10,000 points within the given frequency range. In addition, the distribution of frequency steps is compared directly within Fig. 3 (bottom). The given spacing options within the FEA, namely linear and logarithmic range, mode-based as well as spread spacing, are described in detail in the following.

First, either a continuous *linear* (red) or a *logarithmic* (blue) spacing within the frequency *range* (+) is clearly underestimating the significant contributions of the resonances due to the low frequency resolution. For coarse step sizes frequency steps at the resonances and close by are missing. Further increasing the number of frequency points with these spacing options leads to an appropriate amount results in over-resolved peaks at high frequencies for linear spacing as well as for peaks at low frequencies for logarithmic spacing. Thus, either an inaccurate solution, an excessive computation or a combination of both is expected here [33].

In contrast, the available *mode-based* spacing (•) forces one frequency step exactly at each of the resonances assuring to capture the most significant modal contributions. The given number of frequency steps than is can linearly (red) and thus equidistant or logarithmically (blue) distributed. The frequency resolution with a fixed number of frequency steps for every mode is than depending on the difference between the modal frequencies only. Moreover, the biasing option allows concentrating the frequency steps close to the eigenfrequencies (e.g. bias = 3 in green). In summary, mode-based spacing again may cause conflictive definitions. Assuming a constant number of frequency steps per mode, a high

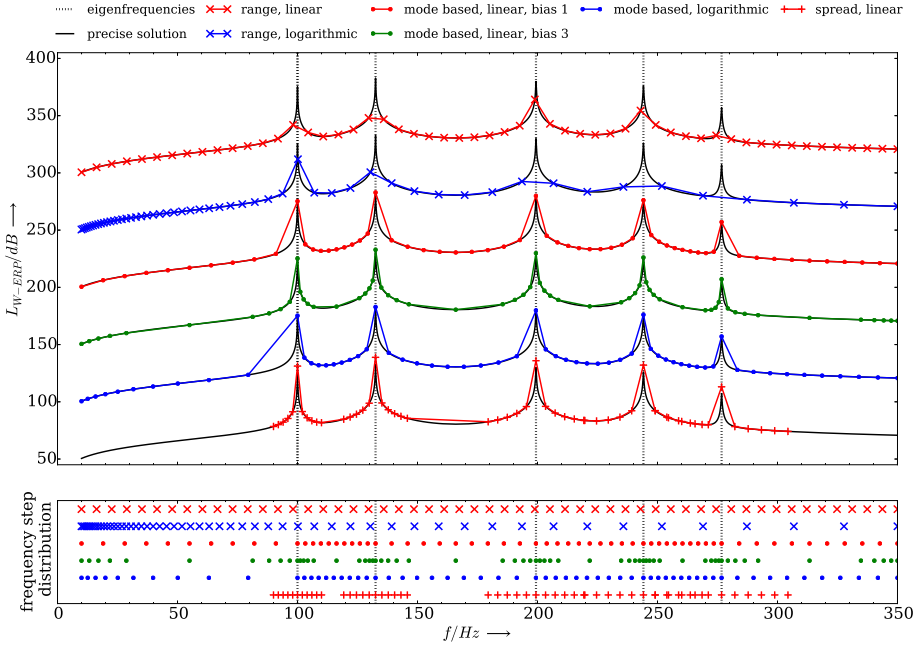


**Fig. 3.** Results of steady state FEA with different frequency step definitions: sound power estimations each overlaying an exact solution with high frequency resolution, offset of 50 dB between the curves due to readability (top) and frequency step distributions (bottom); color scheme: reference solution (black), linear frequency step distribution with bias 1 (red), linear frequency step distribution with bias 3 (green), logarithmic frequency step distribution (blue); in combination with makers for different spacing options: range (*x*), mode-based (•) and spread (+). (For interpretation of the references to colour in this figure legend, the reader is referred to the web version of this article.)

frequency resolution can be achieved on the one hand as the modal density is increasing for higher frequencies (Fig. 2) or two modes occasionally may appear closely. On the other hand, an inappropriate spacing is achieved, if neighbouring modes appear with a high distance.

In addition, a frequency *spread* of $f_s = 0.1$ has been used distributing the frequency steps linearly within $\pm 10\%$ of the related eigenfrequency. Spread-based step definitions might fail for high modal densities with significant overlapping of neighbouring spreads. Then, an unnecessarily high resolution is achieved for less contributing frequencies between the modes which again is inefficient (e.g. Fig. 3: 250–280 Hz).

The constant quality factor

$$Q = \frac{f_0}{\Delta f} = \frac{1}{2D} \tag{18}$$

describing the sharpness of the resonance at $f_0$ with a viscous damping $D$ is commonly determined by the half-power band width (3 dB bandwidth) $\Delta f$. The quality factor has been used in previous studies to achieve an efficient but accurate frequency resolution within a wide frequency range [28,33]. There, at least *five* points per mode have been used to discretise the half-power band of a single mode.

In summary, the available options for the frequency spacing are all quite simple and all yield to certain limitations, either due to a low accuracy, high computational efforts or even both. An adaptive interpolation routine is further introduced and likely to be much more accurate and efficient. This approach is based on the mode-based spacing option with biasing but will focus on an adaptive number of frequency steps.

## 4. Convergence analysis of sound power determination

### 4.1. Convergence analysis: sound radiation of a single mode

In the following, a single mode of the plate is investigated to determine the required frequency spacing parameters. Therein, the general aim is to define a frequency range around each mode being broad enough to consider the modal contribution completely using the least possible number of frequency points.

Thus, the basic question for spread-based frequency step size is an appropriate definition of the required frequency range including most of the radiated sound by choosing the correct spread factor

$$s = \frac{(f_u - f_l)}{f_0} = \frac{1}{Q}. \tag{19}$$

For this purpose, the first torsional mode of the plate at 100 Hz has been investigated. As the sharpness of the peak is depending on the damping, the required spread factor

$$s = \frac{h \cdot \Delta f}{f_0} \quad \text{with} \quad h = [1, 1000] \tag{20}$$

for various frequency ranges $h \cdot \Delta f$ is related to the half-power bandwidth of the mode to be able to transfer the results to every resonance frequency. In this study. the evaluated frequency spread is chosen in a range of 1–1000 times the half-power bandwidth. Thus, the following results are independent of the specific material damping (0.0001 here) or quality factor (5000).

In addition, the number of frequency steps $N_f$ within the frequency range has been varied from 3, which is the least valid value, to 10,000. Last, biasing allows a compression of the points near the resonance as well as an expansion in the frequencies in higher distance. The frequency $f_n$ than is given by

$$f_n = \frac{1}{2}(f_u + f_l) + \frac{1}{2}(f_u - f_l) \cdot |y|^{1/b} sign(y) \quad \text{with} \quad y = -1 + 2\frac{(n-1)}{N_f - 1} \tag{21}$$

The bias parameter $b$ is an exponent and thus chosen between 1 (equidistant spacing) and 3 (default value).

As the improper integral over the area beneath the sound power spectrum over frequency (as in Fig. 1) is infinite, convergence can only be achieved in a defined frequency range of interest. Therefore, the mean power levels (14) are estimated assuring a frequency range being broad enough to represent all of the radiated sound (Fig. 4). The results are shown and discussed for the ERP approximation only. Both, the LPM as well as the kinetic energy achieve exactly the same convergence behaviour.

The most accurate sound power determination is assumed to be for a configuration of h = 1000, bias 3.0 and 10,000 points leads to a reference value of 89.23 dB.

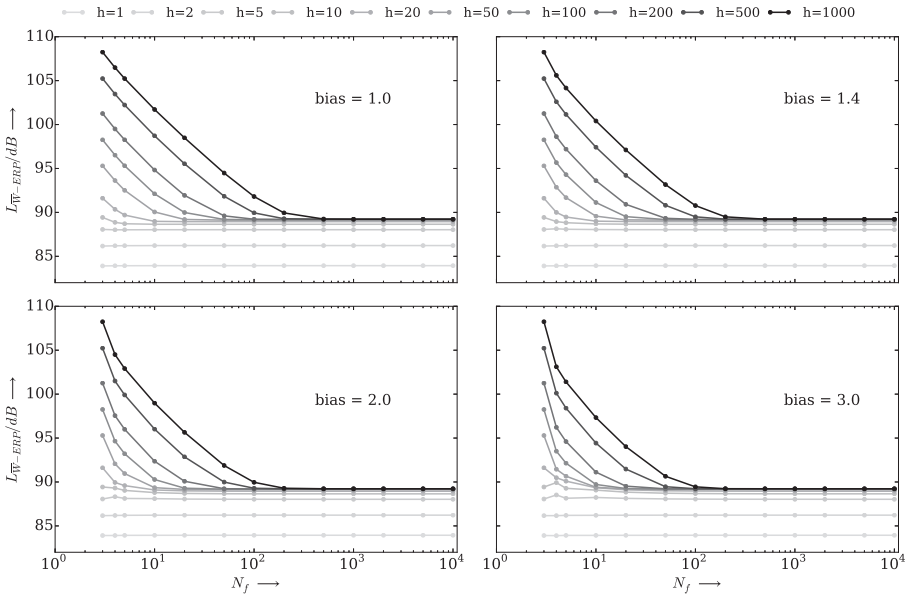


**Fig. 4.** Mean power radiated by the first mode of a rectangular plate: dependency on frequency range and number of frequency steps for different bias parameters.

Fig. 4 illustrates a contradictory convergence: analysing only a narrow frequency range around the mode will underestimate the total power. In contrast, using a broad frequency range around the mode tends to an overestimation for low $N_F$ followed by a convergence against the exact solution. Thus, the deviation of the mean sound power level $\Delta L_{\overline{W}}$ is further understood as the difference of any solution to the most accurate solution. Fig. 5 summarises the convergence of the parameter study using the deviation and introducing a 0.1 dB as well as a 0.5 dB criterion (dark/light green).

Assuming a suitable deviation $\Delta L_{\overline{W}} < 0.5$ dB, convergent results are achieved for a frequency range of at least 20 times the half-power band width ($h > 20$). In detail, for *equidistant* modal spacing the results seem to be satisfying for $N_f > h/3$. Biasing helps to achieve convergence for less frequency steps whereas high bias factors require wide frequency ranges ($h \geqslant 100$). In summary, a relation of

$$N_f > \frac{h}{3\ b} \quad \text{for} \quad \Delta L_{\overline{W}} < 0.5 dB \tag{22}$$

can be given as a rule of thumb to estimate the required frequency steps for a single mode.

A more restrictive deviation criterion of $\Delta L_{\overline{W}} < 0.1$ dB, requires a more broad frequency range of $h > 50$ with similarly using

$$N_f > \frac{h}{2\ b} \quad \text{for} \quad \Delta L_{\overline{W}} < 0.1 \text{ dB} \tag{23}$$

to determine the number of required frequency steps for one mode.

Due to (20), the mentioned frequency spread being broad enough to capture the total modal contribution can be directly related to the viscous damping. As a result a relations

$$s > 20D \quad \text{for} \quad \Delta L_{\overline{W}} < 0.5 \text{ dB} \tag{24}$$

$$s > 50D \quad \text{for} \quad \Delta L_{\overline{W}} < 0.1 \text{ dB} \tag{25}$$

should be considered for an appropriate specification of the frequency range to achieve the accurate mean power results.

### 4.2. Guidelines for mode-based frequency spacing with multiple contributing modes

To define an accurate spacing, the required frequency step has to be related to the distance between two modes $(f_m - f_{m-1})$. Therefore, the given example of the rectangular plate has been further investigated considering all modes in the audible frequency range (see Fig. 2) and used to illustrate this relation.

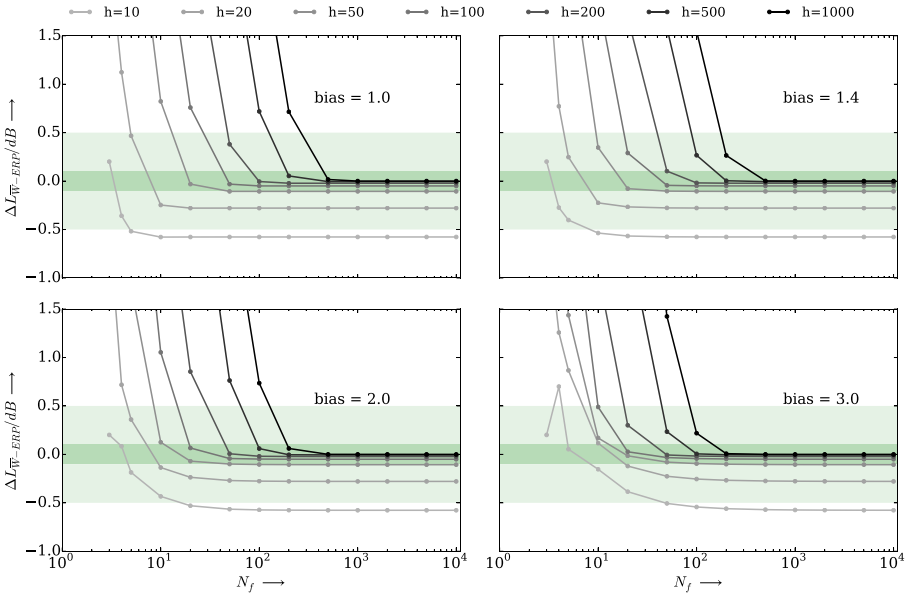


**Fig. 5.** Deviation of the mean power radiated by the first mode of a rectangular plate related to an accurate solution ($N_f = 10^4, h = 1000, b = 3$): dependency on frequency range and number of frequency steps for different bias parameters within a deviation of the mean power of 0.1 dB (dark green) and 0.5 dB (light green). (For interpretation of the references to colour in this figure legend, the reader is referred to the web version of this article.)

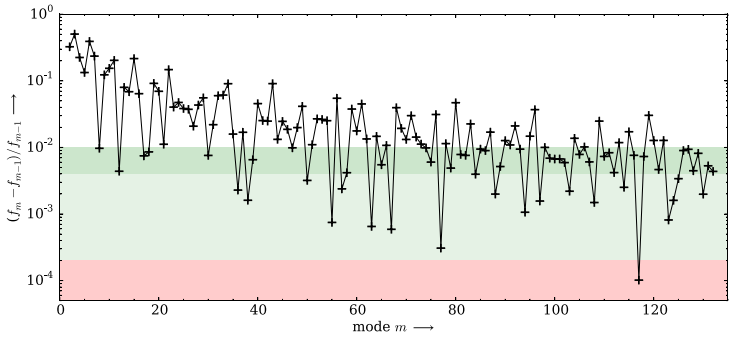


**Fig. 6.** Modal analysis of the rectangular plate: relative distance of eigenfrequencies within $s > 20D$ (light green) and within $s > 50D$ (green) as well as modal interaction (red) for $D = 0.0001$.

Narrow modes may be close enough to automatically fulfil the spread. This is highlighted in Fig. 6 with light green for the 0.5 dB mean power criterion as with dark green for additional modes within the 0.1 dB mean power deviation. A white background represents the modes where spread-based frequency stepping is more efficient than mode-based. At some point, high modal overlap may occur and resolving single modes is not useful any more. Thus, a red background is drawn for the modes overlapping within their half power band width. For the given example, there is only one modal interaction found.

It should be mentioned that this figure is valid for one specific modal damping (D = 0.0001 here). Higher damping would shift the green domain to higher modal distances.

Moreover, the spacing rules for a single mode (22) and (23) as well as the determined modal distances have been combined. Thus, the minimum number of frequency steps of mode $f_m$

$$N_{f\,m} > \frac{6}{D_m b_m} \max\left[\frac{f_m - f_{m-1}}{f_m}, \frac{f_{m+1} - f_m}{f_m}\right] \quad \text{for} \quad \Delta L_{\overline{W}} < 0.5\,\text{dB} \qquad (26)$$

$$N_{f\,m} > \frac{4}{D_m b_m} \max\left[\frac{f_m - f_{m-1}}{f_m}, \frac{f_{m+1} - f_m}{f_m}\right] \quad \text{for} \quad \Delta L_{\overline{W}} < 0.5\,\text{dB} \qquad (27)$$

is estimated using all relevant modal spacing parameters and comparing both neighbouring modes whereas the bigger distance is relevant.

As biasing is recommended to achieve a higher resolution at the sharp resonances, the results of (22) and (23) are shown in Fig. 7 with $b = 3$. It can be observed, that the number of frequency steps is critical especially for low modal densities in the low frequency domain in combination with low damping. In addition, less biasing will increase $N_f$, too.

In the given example, low frequency modes require resolutions of order $10^2$ whereas less than 30 steps are to be applied for mid and high frequencies.

Last, the radiation in the entire frequency range is dominated by some low frequency modes (Fig. 7). In this case, these modes require the highest number of frequency steps, too. Thus, the modal contributions have to be considered for the spacing in a wide frequency domain further on.

### 4.3. Application to full frequency range analysis

Last, the given plate example has been investigated within the entire audible frequency range covering all 132 modes (compare Fig. 2). Lacking free frequency step definitions in the software, the spacing has been applied with equal bias and number of frequency steps for all modes.

Fig. 8 shows a convergence study of the mean power radiated in the frequency range for a different number of frequency steps per mode as well as biasing up to 10. The results are related to a solution with high computational costs ($N_f = 1000, b = 3$). Thus, the previously determined error tolerance of less than 0.1–0.5 dB per mean power of a single mode is accumulated for all modes and thus a deviation to the reference solution of 0.5 and 1 dB is highlighted.

Due to the dominant low frequency modes requiring high modal resolutions, accurate solutions can be achieved for $b > 2$ as well as $N_f > 50$ only.

A huge number of frequency steps leads to significant computational costs. Regarding Fig. 9, the efforts linearly increase with $N_f$. Thus, an adequate spacing helps directly to reduce the total number of evaluation frequencies and thus the total computation efforts.

In addition, significant savings can be achieved for qualitative studies and optimisation procedures on thin-walled components avoiding the computationally expensive acoustic post-processing of the structural dynamic FEA by using the implicitly given kinetic energy only [34].

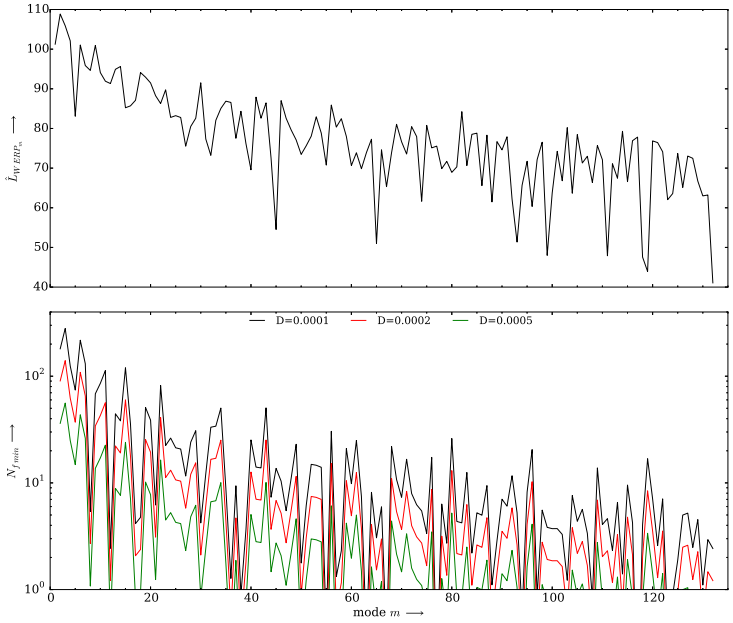


**Fig. 7.** Radiated sound power at each resonance (top) as well as minimum number of frequency steps for an accurate sound power determination of the different modes of the rectangular plate for various damping coefficients using $b = 3$ (bottom).

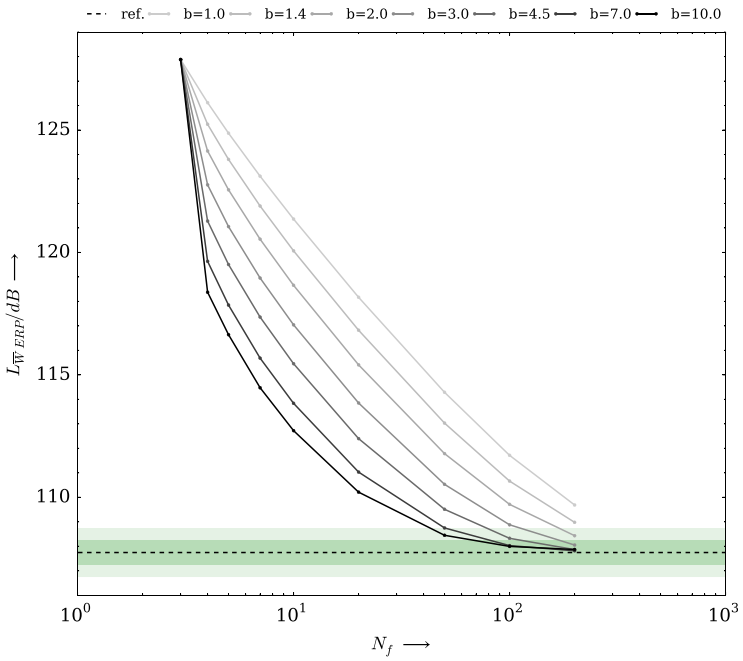


**Fig. 8.** Mean sound power radiated by the all audible modes of a rectangular plate: dependency on number of frequency steps and bias parameters; dotted horizontal line: mean power of an accurate solution ($N_f = 10^3, b = 3$); deviation of the mean power within 0.5 dB (dark green) and 1.0 dB (light green).

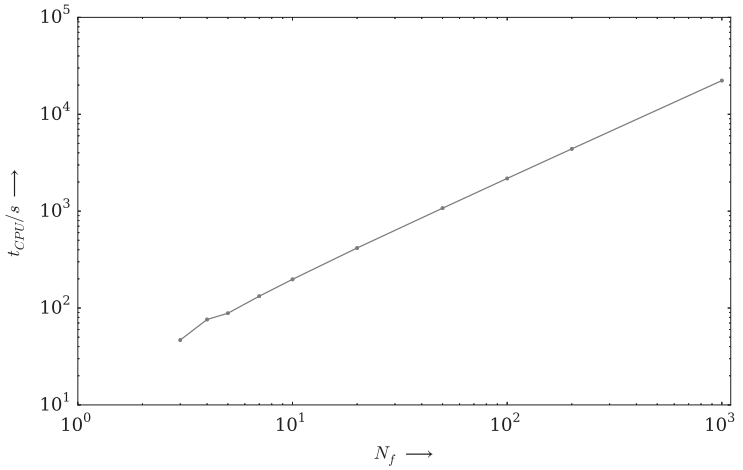


**Fig. 9.** Total cpu time for the steady state FEA of 132 modes of the rectangular plate for different number of frequency steps per mode.

## 5. Conclusions

Within this study, structural steady state FEA and further surface velocity-based sound power approaches have been applied to determine the structure borne sound. Using mode-based model reduction, damping and frequency spacing with biasing, this leads to non-equidistant frequency steps throughout the frequency domain. To achieve a scalar objective of the frequency-dependent sound power, the average power in the given frequency range is determined based on the power spectral density. This approach is independent of the number of modes and frequency steps and valid for varying frequency step sizes and enables the implementation as an optimisation objective.

The steady state FEA is based on a previous modal analysis and using a mode-based frequency spacing with at least one step exact on each of the resonance points. Thus, the total number of frequency steps depends on the number of modes within the treated frequency range, the modal damping as well as biasing. In contrast, basic linear step definitions within a given range may cause a significant underestimation of the sound power by missing the resonance peaks. Despite, spread-based step definitions might be inefficient for high modal densities with overlapping frequency spreads.

The radiated sound of a single mode of a rectangular plate is used to demonstrate convergence concerning the number of required frequency steps. In general, accuracy and efforts are contradictory goals in iterative computations. The given rules should help to reduce the computational expense to a minimum. As a result, a relation to estimate the required frequency spacing of single mode is presented depending on the distance of neighbouring modes as well as damping and biasing. Related to modal density, a recommendation for a common spacing rule is given.

Further studies will address common thin-walled parts besides the academic plate case and include the acoustic quantity in optimisation objectives. Besides, an efficient approach of the frequency integral as a weighted sum over the input mobility using computations at complex frequencies and thus shifting the problem to the complex frequency plane [35,36] may be tested. Another enhancement is the application of a functionality-based approach of adaptive integration techniques, e.g. based on Gauß-Legendre polynomials.

## Acknowledgments

The paper arose in the context of the project DFG-KR 1713/18-1 *Schallabstrahlung bei nichtlinearem und lokal variierendem Dämpfungsverhalten von Mehrlagenverbunden* as well as the Federal Cluster of Excellence EXC 1075 *MERGE Technologies for Multifunctional Lightweight Structures* supported by the Deutsche Forschungsgemeinschaft (DFG). Financial support is gratefully acknowledged.

Furthermore, the critical review of the manuscript by our former colleague Gert Rosenbaum is appreciated.

## Appendix A. Supplementary data

Supplementary data associated with this article can be found, in the online version, athttps://doi.org/10.1016/j.apacoust.2018.09.008.

## References

[1] Ganguli R. Optimum design of a helicopter rotor for low vibration using aeroelastic analysis and response surface methods. J Sound Vib 2002;258(2):327–44.
[2] Narita Y. Layerwise optimization for the maximum fundamental frequency of laminated composite plates. J Sound Vib 2003;263(5):1005–16.
[3] Denli H, Sun J. Structural-acoustic optimization of sandwich structures with cellular cores for minimum sound radiation. J Sound Vib 2007;301(1–2):93–105.
[4] Marburg S. Developments in structural-acoustic optimization for passive noise control. Arch Comput Methods Eng 2002;9:291–370.
[5] Marburg S, Shepherd MR, Hambric SA. Engineering virboacoustic analysis: methods and applications. John Wiley and Sons; 2016 [Ch. Structural-Acoustic Optimization].
[6] Cremer L, Heckl M, Petersson B. Structure-borne sound. Berlin Heidelberg: Springer; 2005.
[7] Mechel FP, editor. Formulas of acoustics. Berlin, Heidelberg: Springer-Verlag; 2008.
[8] Täger O, Dannemann M, Hufenbach WA. Analytical study of the structural-dynamics and sound radiation of anisotropic multilayered fibre-reinforced composites. J Sound Vib 2015;342:57–74.
[9] Marburg S, Nolte B, editors. Computational acoustics of noise propagation in fluids – Finite and boundary element methods. Berlin, Heidelberg: Springer-Verlag; 2008.
[10] Fritze D, Marburg S, Hardtke H-J. Estimation of radiated sound power: a case study on common approximation methods. Acta Acustica United Acustica 2009;95:833–42.
[11] Klaerner M, Wuehrl M, Marburg S, Kroll L. Efficient FEA simulation of structure borne sound radiation. In: Awrejcewicz J, Kazmierczak M, Mrozowski J, Olejnik P, editors. Dynamical Systems – Mathematical and Numerical Approaches. p. 279–90.
[12] Klaerner M, Wuehrl M, Kroll L, Marburg S. Fea-based methods for optimising structure-borne sound radiation. Mech Syst Signal Process 2017;89:37–47.
[13] Finegan IC, Gibson RF. Recent research on enhancement of damping in polymer composites. Compos Struct 1999;44(2–3):89–98.
[14] Ulke-Winter L, Klaerner M, Kroll L. Determining the damping behavior of fiber reinforced composites. Compos Struct 2013;100:34–9.
[15] Sepahvand K. Spectral stochastic finite element vibration analysis of fiber-reinforced composites with random fiber orientation. Compos Struct 2016;145:119–28.
[16] Marburg S, Beer H-J, Gier J, Hardtke H-J, Rennert R, Perret F. Experimental verification of structural-acoustic modelling and design optimisation. J Sound Vib 2002;252(4):591–615.
[17] Billups E, Cavalli M. 2d damping predictions of fiber composite plates: layup effects. Compos Sci Technol 2008;68(3–4):727–33.
[18] Saravanos DA, Chamis CC. Unified micromechanics of damping for unidirectional fiber reinforced composites, NASA Technical Memorandum 102107 (08 1989).
[19] Adams RD, Maheri MR. Damping in advanced polymer-matrix composites. J Alloys Compounds 2003;355(1–2):126–30.
[20] Klaerner M, Wuehrl M, Kroll L, Marburg S. Modelling and fea-simulation of the anisotropic damping of thermoplastic composites. Adv Aircraft Spacecraft Sci 2016;3(3):331–49.
[21] Roozen-Kron PJM. Structural optimization of bells. Technische Universiteit Eindhoven; 1992 (Ph.D. thesis).
[22] Kinsler LE, Frey AR, Coppens AB, Sanders JV. Fundamentals of acoustics. Wiley; 2000.
[23] Koopmann GH, Fahnline JB. Designing quiet structures. London: Academic Press; 1997.
[24] Fahnline J, Koopmann G. A lumped parameter model for the acoustic power output from a vibrating structure. J Acoust Soc Am 1996;100(6):3539–47.
[25] Fahnline J, Koopmann G. Numerical implementation of the lumped parameter model for the acoustic power output of a vibrating structure. J Acoust Soc Am 1997;102(1):179–92.
[26] Luegmair M, Münch H. Verbesserte Equivalent Radiated Power (ERP) Berechnung, in: DAGA 2015–41. Jahrestagung für Akustik, 2015, pp. 834–36.
[27] Dassault Systemes, Abaqus 6.14 Theory Guide; 2014.
[28] Shepherd MR, Hambric SA. Minimizing the acoustic power radiated by a fluid-loaded curved panel excited by turbulent boundary layer flow. J Acoust Soc Am 2014;136(5):2575–85.
[29] Press WH, Teukolsky SA, Vetterling WT, Flannery BP. Numerical recipes 3rd edition: the art of scientific computing. 3rd edition. New York, NY, USA: Cambridge University Press; 2007.
[30] Davis PJ, Rabinowitz P, editors. Methods of numerical integration. Edition: Academic Press; 1984.
[31] Krylov VI, Stroud AH. Approximate calculation of integrals. Dover Publications Inc.; 2006.
[32] Langer P, Maeder M, Guist C, Krause M, Marburg S. More than six elements per wavelength: the practical use of structural finite element models and their accuracy in comparison with experimental results. J Comput Acoust 2017;25:1750025.
[33] Shepherd M. Structural-acoustic optimization of structures excited by turbulent boundary layer flow. Pennsylvania State University; 2014 [Ph.D. thesis].
[34] Klaerner M, Marburg S, Kroll L, FE-based measures for structure borne sound radiation. In: inter.noise 2014: 43rd International Congress on Noise Control Engineering, Melbourne, Australia; 2014.
[35] D'Amico R, Koo K, Huybrechs D, Desmet W. On the use of the residue theorem for the efficient evaluation of band-averaged input power into linear second-order dynamic systems. J Sound Vib 2013;332(26):7205–25.
[36] D'Amico R, Huybrechs D, Desmet W. A refined use of the residue theorem for the evaluation of band-averaged input power into linear second-order dynamic systems. J Sound Vib 2014;333(6):1796–817.